The pressure–temperature phase diagram of $BaTiO_3$: a macroscopic description of the low-temperature behaviour

2002 J. Phys.: Condens. Matter 14 L599

(http://iopscience.iop.org/0953-8984/14/36/101)

INSTITUTE OF PHYSICS PUBLISHING JOURNAL OF PHYSICS: CONDENSED MATTER

J. Phys.: Condens. Matter **14** (2002) L599–L604 PII: S0953-8984(02)38227-4

LETTER TO THE EDITOR

The pressure–temperature phase diagram of $BaTiO_3$: a macroscopic description of the low-temperature behaviour

S A Hayward and E K H Salje

Department of Earth Sciences, University of Cambridge, Downing Street, Cambridge CB2 3EQ, UK

E-mail: sah21@esc.cam.ac.uk

Received 17 June 2002
Published 29 August 2002
Online at stacks.iop.org/JPhysCM/14/L599

Abstract

The pressure–temperature phase diagram of $BaTiO_3$ has been investigated using a modification of the standard Landau potential to take account of quantum saturation of the order parameter at low temperatures. The calculated phase diagram agrees well with experiment for the cubic–tetragonal and tetragonal–orthorhombic transitions, but underestimates the orthorhombic–rhombohedral transition temperature somewhat. The saturation temperature ($\theta_S = 160$ K) is sufficiently high that the expected critical point is not observed experimentally. Instead, each phase boundary bends sharply down, so each of the four crystalline structures of $BaTiO_3$ has a stability field with increasing pressure at 0 K.

1. Introduction

$BaTiO_3$ undergoes a sequence of ferroelectric phase transitions on cooling, from the cubic perovskite aristotype structure, through tetragonal, orthorhombic and finally rhombohedral structures. These phase transitions can be modified by a wide range of secondary variables, such as chemical doping, electrical and mechanical stress fields, and hydrostatic pressure; see the reviews by Jona and Shirane (1962) and Lines and Glass (1977). Here we are concerned with the phase diagram of $BaTiO_3$ as a function of pressure and temperature, with particular focus on the relative stability of the various phases at low temperature. This work follows the first experimental study of the low-temperature part of the phase diagram by Ishidate *et al* (1997) and the recent first-principles calculations of the $BaTiO_3$ phase diagram by Íñiguez and Vanderbilt (2002). In this letter, we use a macroscopic Landau potential to describe the sequence of phase transitions in $BaTiO_3$.

As well as being used as a ferroelectric material, $BaTiO_3$ has played an important role in the development of our theoretical understanding of ferroelectric phase transitions. An important landmark in the theory of $BaTiO_3$ was the application of a polynomial-type free

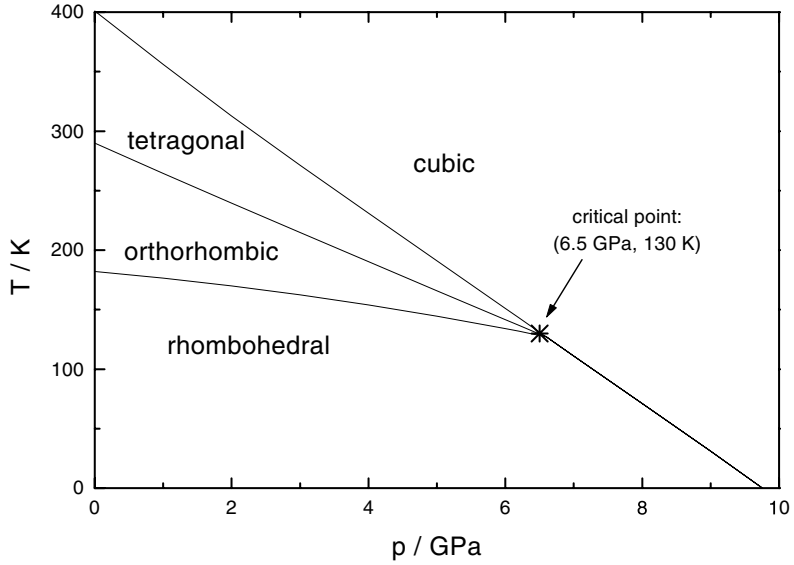

Figure 1. The pressure versus temperature phase diagram for $BaTiO_3$, based on low-pressure experiments and classical extrapolation (Samara 1966, 1971, Decker and Zhao 1989).

energy expression (nowadays commonly described as a Landau potential) to describe the sequence of phases at ambient pressure (Devonshire 1949, 1951). As well as relating the thermal, structural and dielectric anomalies to each other, this model showed that the various transitions were described consistently by a single underlying free energy function.

The different phases of $BaTiO_3$ are a system with a degenerate order parameter; a single order parameter (essentially the displacement of the Ti from the centre of its octahedral coordination polyhedron) can initially act along one of three perpendicular directions. The subsequent phase transitions occur as the second and third components of the order parameter vector are activated.

The initial model of Devonshire was extended by Forsbergh (1954) to include the effects of two-dimensional and hydrostatic pressures. The effect of a secondary field on the phase transition is conveniently incorporated into a Landau model, by introducing terms describing the coupling between the order parameter and the applied field. The precise form of the couplings is determined by the change in crystal structure at the phase transition, the key aspects being the point groups of the two structures, and whether there is doubling of the unit cell at the transition. These factors determine the coupling between the order parameter and the spontaneous strain (see Stokes and Hatch (1988) for a description of these relationships) which in turn determines how the free energy is affected by mechanical stress.

The low-pressure part of the phase diagram was measured using dielectric measurements by Samara (1966, 1971), and was found to be consistent with a classical Landau model of the type developed by Forsbergh (1954). Extrapolating the phase diagram to higher pressures was expected to lead to one or two critical points (figure 1). However, when the high-pressure experiments were performed (Ishidate *et al* 1997), it was found that the phase diagram did not have any critical points (figure 2). Instead, each phase boundary became quadratic, rather than linear, with increasing pressure. This result is characteristic of a phase transition modified by quantum mechanical effects.

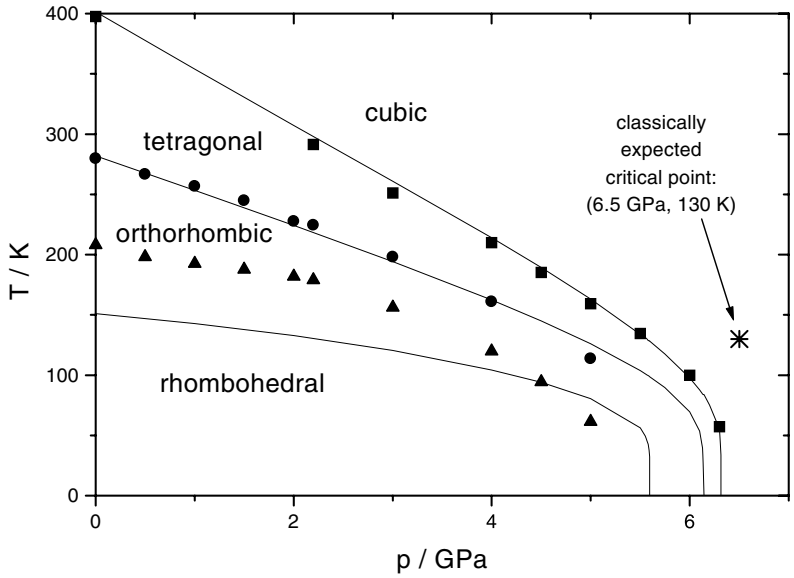

Figure 2. The pressure versus temperature phase diagram for $BaTiO_3$, showing experimental data over the entire pressure range (Ishidate *et al* (1997): ■: cubic–tetragonal; ●: tetragonal–orthorhombic; ▲: orthorhombic–rhombohedral). The solid curves show the phase fields calculated in the text.

2. The model

The classical Landau potential, $\Delta G = (A/2)(T - T_C)Q^2 + (B/4)Q^4 + (C/6)Q^6 + \cdots$, has been shown to follow from the general ϕ^4-model in the displacive limit at high temperatures (Salje *et al* 1991). Removing the high-temperature constraint leads, for Einstein modes with relatively flat dispersion of the soft mode, to a more general result, $\Delta G = (A/2)(\theta_S \coth(\theta_S/T) - \theta_S \coth(\theta_S/T_C))Q^2 + (B/4)Q^4 + (C/6)Q^6 + \cdots$, where θ_S is a saturation temperature, below which quantum mechanical effects are important. Even more general solutions are discussed by Salje *et al* (1991) and Pérez-Mato and Salje (2001). Although this $\coth(\theta_S/T)$ solution is only strictly correct for certain soft-mode dispersions and hard-mode couplings, it is a good approximation in the general case. Away from the displacive limit, the free energy expansion automatically contains a sixth-order term. At least at low pressures, the mechanism of the transition in $BaTiO_3$ has a significant order–disorder aspect, as evidenced by EPR studies of the local structure of $BaTiO_3$ at ambient pressure (Müller and Berlinger 1986).

The effect of secondary fields can be added to the quantum mechanical Landau potential in the same way as for the classical potential. Hayward and Salje (1998) used this method to model the variation of the transition temperature with variables such as composition, pressure and uniaxial stress for a range of phase transitions with a single order parameter. Here, we take this approach to describe the (pressure, temperature) phase diagram of $BaTiO_3$ at high and low temperatures.

The starting point is the classical Devonshire (1949, 1951) model of $BaTiO_3$ at zero pressure;

$$\Delta G = \frac{A}{2}(T - T_C)(Q_1^2 + Q_2^2 + Q_3^2) + \frac{B}{4}(Q_1^4 + Q_2^4 + Q_3^4) + \frac{B'}{2}(Q_1^2Q_2^2 + Q_2^2Q_3^2 + Q_1^2Q_3^2) + \frac{C}{6}(Q_1^6 + Q_2^6 + Q_3^6) \quad (1)$$

with $A = 4.53\,\mathrm{J\,K^{-1}\,mol^{-1}}$, $B = -787.8\,\mathrm{J\,mol^{-1}}$, $B' = 945.36\,\mathrm{J\,mol^{-1}}$, $C = 2568.8\,\mathrm{J\,mol^{-1}}$, $T_C = 391$ K. By definition, the tetragonal phase has $Q_1 \neq 0$, $Q_2 = Q_3 = 0$. Similarly, the orthorhombic phase has $Q_1 = Q_2 \neq 0$, $Q_3 = 0$ and the rhombohedral phase has $Q_1 = Q_2 = Q_3 \neq 0$. Equation (1) can therefore be rewritten in three separate forms, to give the free energy difference between the cubic phase and each of the tetragonal, orthorhombic and rhombohedral phases.

Each of these expressions is a simple Landau potential, so it is routine to determine the equilibrium value of Q for each phase, and the associated value of the excess free energy ΔG, at any temperature T. The equilibrium phase will of course be the one with the lowest ΔG, and phase transitions occur when two of the phases have the same value of ΔG. For the cubic–tetragonal transition, the equilibrium transition temperature is found by equating the excess free energy of the cubic phase ($Q = 0$ and hence $\Delta G = 0$) with that of the tetragonal phase (Q is at the minimum of $G(Q)$), leading to the standard result,

$$T_{TR} = T_C + \frac{3B^2}{16AC}. \tag{2}$$

For the tetragonal–orthorhombic and orthorhombic–rhombohedral transitions, it is necessary to determine the transition temperature numerically, but the underlying method is the same.

The couplings between the spontaneous strains and the order parameters are of the forms $e_i Q_i^2$ and $e_i(Q_j^2 + Q_k^2)$, and so the lowest-order coupling terms require pressure dependences in the Q_i^2, Q_i^4 and $Q_i^2 Q_j^2$ terms of equation (1):

$$\begin{aligned}\Delta G = {} & \frac{A}{2}(T - T_C)(Q_1^2 + Q_2^2 + Q_3^2) + \frac{B}{4}(Q_1^4 + Q_2^4 + Q_3^4) \\ & + \frac{B'}{2}(Q_1^2Q_2^2 + Q_2^2Q_3^2 + Q_1^2Q_3^2) + \frac{C}{6}(Q_1^6 + Q_2^6 + Q_3^6) \\ & + \kappa_1 p(Q_1^2 + Q_2^2 + Q_3^2) + \kappa_2 p(Q_1^4 + Q_2^4 + Q_3^4) + \kappa_3 p(Q_1^2Q_2^2 + Q_2^2Q_3^2 + Q_1^2Q_3^2),\end{aligned} \tag{3}$$

which simplifies to

$$\begin{aligned}\Delta G = {} & \frac{A}{2}(T - T_C + \lambda_1 p)(Q_1^2 + Q_2^2 + Q_3^2) + \frac{B(1 + \lambda_2 p)}{4}(Q_1^4 + Q_2^4 + Q_3^4) \\ & + \frac{B'(1 + \lambda_3 p)}{2}(Q_1^2Q_2^2 + Q_2^2Q_3^2 + Q_1^2Q_3^2) + \frac{C}{6}(Q_1^6 + Q_2^6 + Q_3^6).\end{aligned} \tag{4}$$

To determine the parameters of this classical Landau potential, the zero-pressure results of Devonshire (1949) were used for A, B, C and T_C. The value of λ_1 was found by fitting the gradient of the experimental cubic/tetragonal phase boundary of Ishidate *et al* (1997) at low pressures. The parameter λ_2 is constrained by the observation that the cubic–tetragonal phase transition has a tricritical point at $p_T = 3.5$ GPa, $T = 233$ K (Decker and Zhao 1989), which implies that the prefactor of Q_1^4 in equation (4) is zero when $p = p_T$. The effect of λ_3 is to cause the transition temperatures for the tetragonal–orthorhombic and orthorhombic–rhombohedral transitions to be more weakly pressure dependent than for the cubic–tetragonal transition. Given the value of λ_1, λ_3 was fitted to the gradient of the experimental tetragonal/orthorhombic phase boundary at low pressures, as measured by Ishidate *et al* (1997). As noted above, the tetragonal–orthorhombic transition temperature must be determined numerically, as the temperature where the equilibrium values of Q for the orthorhombic and rhombohedral phases have equal values of G. Adjusting λ_3 changes the variation of the transition temperature with pressure. In order to reproduce the observed classical behaviour of $BaTiO_3$ as a function of pressure, $\lambda_1 = -40\ \mathrm{K\,GPa^{-1}}$, $\lambda_2 = -0.286\ \mathrm{GPa^{-1}}$, $\lambda_3 = -0.04\ \mathrm{GPa^{-1}}$. Extrapolated to higher pressures, these parameters lead to the phase diagram in figure 1, which has a critical point.

To incorporate low-temperature effects, we modify the prefactor for the term in Q_i^2 leading, in the limit of an Einstein-type soft mode, to

$$\Delta G = \frac{A}{2}\left(\theta_S \coth\left(\frac{\theta_S}{T}\right) - \theta_S \coth\left(\frac{\theta_S}{T_C}\right) + \lambda_1 p\right)(Q_1^2 + Q_2^2 + Q_3^2) + \frac{B(1+\lambda_2 p)}{4}(Q_1^4 + Q_2^4 + Q_3^4) + \frac{B'(1+\lambda_3 p)}{2}(Q_1^2Q_2^2 + Q_2^2Q_3^2 + Q_1^2Q_3^2) + \frac{C}{6}(Q_1^6 + Q_2^6 + Q_3^6). \quad (5)$$

3. Comparison with experiment

Comparing equations (4) and (5), equation (5) has one additional fit parameter, θ_S. The saturation parameter, $\theta_S = 160$ K, was fitted explicitly to the data for the cubic–tetragonal phase transition, to produce agreement between the calculated cubic–tetragonal transition temperature and the experiments of Ishidate *et al* (1997). The same parameter also gives good agreement for the tetragonal–orthorhombic transition. The experimental orthorhombic–rhombohedral phase boundary agrees less well with the model.

The model used to describe $BaTiO_3$ in this letter emphasizes the displacive aspects of the phase transition. In the case of an order–disorder transition, the model of equation (5) will be modified. One way of visualizing the change is to note that in the high-temperature limit of Landau-type models, the excess entropy associated with the transition $\Delta S \propto Q^2$. For a Bragg–Williams order–disorder process, the configurational excess entropy $\Delta S(\text{config}) \propto (1+Q)\ln(1+Q)+(1-Q)\ln(1-Q)$. Thus the higher-order terms in the free energy polynomial are temperature dependent in an order–disorder transition. This change will affect the phase diagram, but not greatly. For $p > 3.5$ GPa, the cubic–tetragonal phase transition is second order, and so the transition temperature only depends on terms in Q^2. The temperatures of other transitions will be affected by changes in the prefactors of Q^4 and Q^6. However, the values of Q at the transitions become smaller with increasing pressure, which reduces the contribution of the high-order terms to the free energy at the high-pressure/low-temperature end of the phase diagram. Low values of the order parameter are generally favoured at high pressure in $BaTiO_3$, since the off-centring of the Ti cation leads to a clear increase in the specific volume for the cubic–tetragonal and tetragonal–orthorhombic transitions (Shriane and Takeda 1952, Kwei *et al* 1993). For the orthorhombic–rhombohedral transition, the measured volume anomaly at the transition is small, and so even determining its sign is not straightforward (Kwei *et al* 1993). However, since the orthorhombic–rhombohedral transition temperature falls with increasing pressure, the Clausius–Clapeyron equation implies that $\Delta V(\text{orthorhombic} \rightarrow \text{rhombohedral})$ is also positive.

The most significant result seen on comparing the classical (figure 1) and modified (figure 2) phase diagrams is that classical theory does not predict stability fields for the tetragonal or orthorhombic phases as a function of pressure near 0 K. By contrast, including the quantum mechanical modification of Landau theory stabilizes these two phases with respect to the rhombohedral structure. This is consistent with the experimental data of Ishidate *et al* (1997) and the Monte Carlo simulations of Íñiguez and Vanderbilt (2002). The reason that the critical point is lost is that it lies in the temperature range of the phase diagram where $BaTiO_3$ is behaving as a quantum paraelectric; the cubic structure is stabilized by zero-point effects. Similarly, the tetragonal phase is stabilized relative to the orthorhombic phase, which is stabilized relative to the rhombohedral phase.

We thank J M Pérez-Mato for introducing us to this problem, and for other helpful discussions.

References

Decker D L and Zhao Y X 1989 *Phys. Rev.* B **39** 2432
Devonshire A F 1949 *Phil. Mag.* **40** 1040
Devonshire A F 1951 *Phil. Mag.* **42** 1065
Forsbergh P W 1954 *Phys. Rev.* **93** 686
Hayward S A and Salje E K H 1998 *J. Phys.: Condens. Matter* **10** 1421
Íñiguez J and Vanderbilt D 2002 First-principle study of the temperature–pressure phase diagram of $BaTiO_3$ *Phys. Rev. Lett.* at press
(Íñiguez J and Vanderbilt D 2002 *Preprint* cond-mat/0204497)
Ishidate T, Abe S, Takahashi H and Môri N 1997 *Phys. Rev. Lett.* **78** 2397
Jona F and Shirane G 1962 *Ferroelectric Crystals* (Oxford: Pergamon)
Kwei G H, Lawson A C, Billinge S J L and Cheong S-W 1993 *J. Phys. Chem.* **97** 2368
Lines M E and Glass A M 1977 *Principles and Applications of Ferroelectrics and Related Materials* (Oxford: Clarendon)
Müller K A and Berlinger W 1986 *Phys. Rev.* B **34** 6130
Pérez-Mato J M and Salje E K H 2001 *Phil. Mag. Lett.* **81** 855
Salje E K H, Wruck B and Thomas H 1991 *Z. Phys.* B **82** 399
Samara G A 1966 *Phys. Rev.* **151** 378
Samara G A 1971 *Ferroelectrics* **2** 277
Shirane G and Takeda A 1952 *J. Phys. Soc. Japan* **7** 1
Stokes H T and Hatch D M 1988 *Isotropy Subgroups of the 230 Crystallographic Space Groups* (Singapore: World Scientific)